Simple and Reliable Quartz Crystal Microbalance Technique for Determination of Solubility by Cooling and Heating Solution

ARTICLE *in* ANALYTICAL CHEMISTRY · FEBRUARY 2015

Impact Factor: 5.64 · DOI: 10.1021/ac504492g · Source: PubMed

3 AUTHORS, INCLUDING:

Li-Shang Liu

6 PUBLICATIONS **287** CITATIONS

SEE PROFILE

analytical chemistry

Article

pubs.acs.org/ac

Simple and Reliable Quartz Crystal Microbalance Technique for Determination of Solubility by Cooling and Heating Solution

Li-Shang Liu,[†] Jong-Min Kim,[‡] and Woo-Sik Kim*[,†]

[†]Department of Chemical Engineering, Kyung Hee University, Yongin-si, Gyeonggi-do 446-701, South Korea

[‡]Department of Chemical Engineering, Dong-A University, Hadan 840, Saha, Busan 604-741, South Korea

Supporting Information

ABSTRACT: A quartz crystal microbalance (QCM) is presented as a promising technique for determining the solubility and induction of nucleation via the cooling and reverse heating of a solution. When cooling and heating a solution, the resonant frequency (F) and resonant resistance (R) of the QCM responses change significantly due to vibrational loss related to the viscous and elastic friction that depend on the solution viscosity and solid mass on the sensor, respectively. Thus, obvious refraction points appear in the QCM response profile at the induction point of primary nucleation during cooling crystallization and at the saturated point during heating dissolution. Using an $F-R$ plot of the QCM responses, the phase changes between liquid and solid at the induction and saturated points are confirmed. When compared with focused beam reflectance measurement (FBRM) and gravimetric methods, the QCM method is confirmed to be highly accurate and reliable for determining the solubility, making it a highly promising method for determining solubility and crystal nucleation with minimal effort based on simple temperature cycling, thereby avoiding precalibration and sampling.

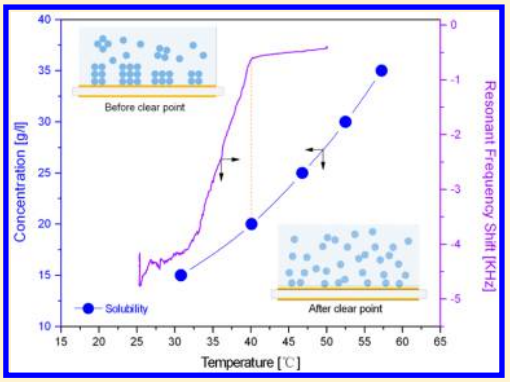

Crystallization is an important unit operation for separation and purification in the chemical, food, and pharmaceutical industries. For precise control of crystallization processes, such as crystal nucleation, growth, size distribution, polymorphs, and so forth, the solubility of the solute provides crucial information. Thus, various attempts have already been made to develop a simple and reliable technique for determining the solubility, where the current methods can be classified as thermodynamic or kinetic.

The kinetic method was developed for a high-throughput determination of solubility in the development of a new drug, in which a dimethyl sulfoxide (DMSO) stock solution is gradually added to the aqueous solute solution until the first solute solid is precipitated to determine the solubility.[1] Yet, despite the advantage of a fast and automated determination process, this method includes inherent drawbacks in determining the solubility due to the DMSO producing a higher value than the true value.[2]

Thus, the thermodynamic method is frequently adopted for an accurate determination of solubility. In this method, enough solute solids are dissolved in the solvent to obtain a saturated solution. This method is also subclassified as a gravimetric, analytical, or synthetic method according to the technique used to determine the concentration of the saturated solution. A gravimetric method is most commonly used due to its high accuracy and simplicity, despite being labor intensive and time-consuming because of sampling, filtering, drying, and weighing.[2] Analytical methods include many techniques depending on the analytical instruments used to determine the solution concentration, such as UV, Raman, IR spectroscopy, and HPLC. However, all analytical methods require accurate precalibration of the instrument. Furthermore, solute compounds which have no double bond (π bond) cannot be analyzed by spectroscopy.[3−6] In the case of synthetic method, the temperature at which the solute solids are completely dissolved is counted as the solubility. Many different techniques have also been developed to monitor the complete dissolution in the solution, including a focused beam reflectance measurement (FBRM) to detect the variation of solid particles,[7] turbidimeter to detect the change of turbidity of the solution,[8] calorimeter to detect the heat release during the dissolution,[9] and refractometer to detect the variation in the refractive index of the solution.[10] As a result, a synthetic method is frequently used for determining the solubility as it can be directly applied to the solution without any pretreatment, such as solid filtration or instrument calibration. However, the accuracy of this type of method is limited due to a low resolution of the detection response to the solid dissolution in the solution and variations in the detection response under heating conditions with certain techniques.

Accordingly, this study presents a new QCM (quartz crystal microbalance) technique for the accurate and reliable

Received: December 2, 2014
Accepted: February 13, 2015
Published: February 13, 2015

DOI: 10.1021/ac504492g
Anal. Chem. 2015, 87, 3329−3335

determination of solubility (saturated concentration). Due to piezoelectricity, the quartz crystal vibrates at a resonant frequency infinitely upon stimulation of an alternative potential.[11] Plus, the resonant frequency varies according to the mass deposited on the crystal and physical property changes around the crystal. Therefore, due to their ultrahigh sensitivity to subtle property changes,[12] QCMs have become an emerging tool for assessing kinetics in the following contexts: atomic layer deposition kinetics,[13] cell growth kinetics,[14] and enzymatic kinetics of cellulose hydrolysis;[15] for detecting molecular recognition, such as chirality discrimination,[16−19] environmental pollutant detection,[20] and cancer biomarker detection;[21] for analyzing conformational arrangement, such as ligand-induced conformational rearrangement in HIV-1 envelope proteins[22] and conformational changes in DNA upon transcription;[23] and for analyzing phase transition, such as the deliquescence phase transition of inorganic films[24] and thermal phase transition phenomena of Langmuir−Blodgett films.[25] In addition, QCMs have a high potential for use in a wide range of applications due to their high detection capability of the property changes in all phases of gas, liquid, and solid, compared with other electrochemical sensors which have a low detection limit and a wide dynamic range.[26−33]

The key strength of a QCM is its ability to simultaneously detect subtle property changes in both solid and liquid phases. As demonstrated in our previous study, a combined nucleation and crystal growth analysis was achieved using a QCM, where the phase transition from liquid to solid was accurately and clearly reflected by a resonant frequency shift, providing metastable zone information during cooling crystallization, whereas the crystal growth rate was reflected based on a further analysis of an $F-R$ plot.[34]

Therefore, this study presents a new QCM technique for determining solubility based on simply cooling and heating the solution. The accuracy and reliability of the solubility determined by the proposed QCM technique are evaluated in comparison with the FBRM and gravimetric methods at various heating rates and solution concentrations.

EXPERIMENTAL SECTION

The sulfamerazine (SMZ) was provided by Sigma-Aldrich with a purity of 99%$^+$. A mixture of acetonitrile and deionized water at 80/20 vol % was prepared as the solvent. As shown in Figure 1a, the temperature for the cooling and heating solution was controlled using a programmable circulator (GR 150 water bath, Grant Instruments, U.K.). A QCM sensor (9 MHz, Princeton Applied Research, U.S.A.), FBRM probe, and thermometer were installed in the crystallizer to *in situ* monitor the property changes of the solution and solid phases. A quartz crystal analyzer (QCA 922, Seiko SG&G, Japan) was used to monitor the resonant frequency and resonant resistance shifts. The FBRM was also applied to monitor the crystal formation and dissolution during the cooling and heating. The cooling process was carried out using the following procedure: (i) a clear SMZ solution of a certain concentration, i.e., 20g/l, was maintained at a high temperature of 50 °C for 30 min; (ii) the SMZ solution was then cooled to 25 °C at a constant cooling rate; and lastly, (iii) the suspension was subjected to a reverse heating process back to the initial high temperature of 50 °C. For the determination of solubility, the SMZ concentration and heating rate were varied. As a reference, the same cooling and heating experiment was carried out using a blank solution without the SMZ solute. Using the *in situ* QCM responses, the solubility of the SMZ and induction point of nucleation were determined and their accuracy was evaluated using the thermogravimetric method (Supporting Information I) and FBRM response.

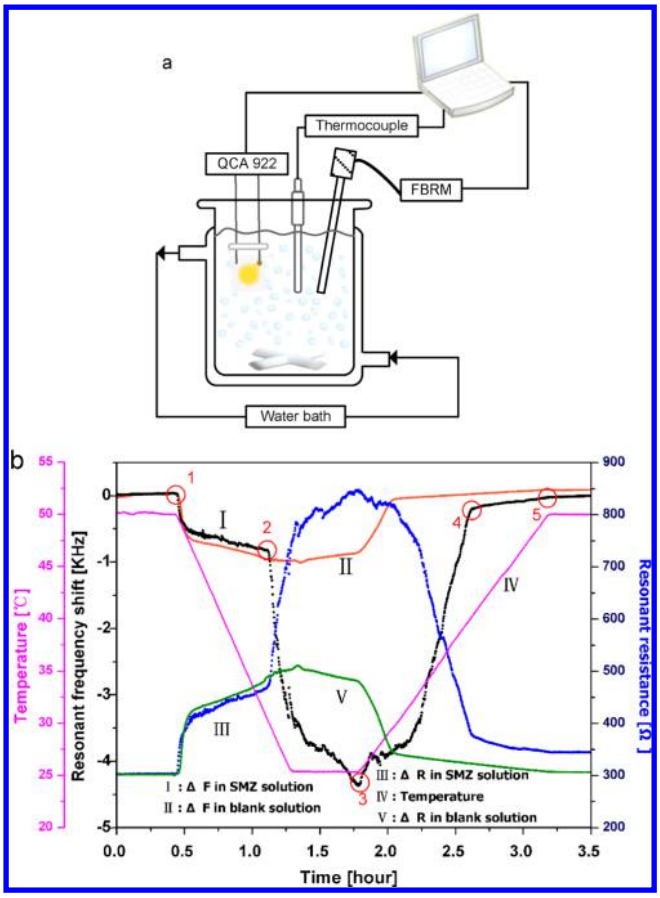

Figure 1. (a) Schematic of experimental system. The resonant frequency and resonant resistance of the QCM sensor were monitored using a QCA 922. The particle number was measured by FBRM. The solution temperature was controlled by a water bath. (b) *In situ* analysis of cooling and heating of solution using QCM: resonant frequency shift in 20g/l SMZ (I); resonant frequency shift in blank solution (II); resonant resistance shift in 20g/l SMZ (III); temperature profile (IV); and resonant resistance shift in blank solution (V).

RESULTS AND DISCUSSION

QCM Responses to Cooling and Heating Solution. Figure 1b shows the QCM responses to the cooling and heating cycle of the SMZ solution (20 g/L) and the blank solution without SMZ. As the blank solution was linearly cooled to 25 °C, the resonant frequency also gradually decreased due to the increased viscosity of the solution (curve II in Figure 1b). In the case of the SMZ solution (20 g/L) (curve I in Figure 1b), the QCM responses were also similar to those in the blank solution until the solution was cooled to the temperature of point 2. However, a dramatic resonant frequency shift was triggered by further cooling due to the induction of crystal nucleation.[34] This significant shift in the resonant frequency then continued during the cooling to 25 °C.

In general, a resonant frequency change of QCM sensor is due to vibrational loss originating from the solution viscosity (called viscous friction) and solid mass (called elastic friction) loaded on the sensor. According to Sauerbrey's equation, a resonant frequency shift due to elastic friction (ΔF_m) is linearly

DOI: 10.1021/ac504492g
Anal. Chem. 2015, 87, 3329−3335

proportional to the amount of mass change on the sensor ($\pm\Delta$m),[35] $\Delta F_m = -C_m\Delta m$, where C_m is the mass-sensitive constant. Meanwhile, a resonant frequency shift due to viscous friction (ΔF_l) depends on the viscosity change of the solution,[36] as $\Delta F_l = -C_l(\rho_L\eta_L)^{1/2}$, where ρ_l and η_l are the density and viscosity of the liquid film, respectively, and C_l is the viscosity-sensitive constant. Here, C_m and C_l were estimated as 0.9153×10^{-9} and 61 000, respectively (See Supporting Information II).

Using the above equations, it was predicted that ΔF_l was gradually increased due to the increased viscosity when cooling the solution and reached about −1.0 kHz at 25 °C (Supporting Information III, Figure S-1). This prediction matched well with the QCM response to the resonant frequency shift in the blank solution during the cooling process (50 °C → 25 °C), indicating that the resonant frequency shift in the blank solution was totally dictated by viscous friction on the sensor because there was no crystal formation.

Similarly, the QCM response (ΔF) in the SMZ solution (20 g/L) matched well with Sauerbrey's equation of ΔF_l until the temperature at point 2, indicating no crystal formation in the solution (Supporting Information III, Figure S-1). In fact, the SMZ solution (20 g/L) below the temperature of point 2 was sufficiently supercooled for crystal nucleation, resulting in solid mass (crystal) loading on the sensor. Thus, if the amount of solid mass loaded on the sensor (Δm) is assumed to be proportional to the supercooling ($\Delta C = C - C_S(T)$), the maximum ΔF_m was predicted to be about −3.0 kHz during the cooling to 25 °C. This prediction also matched well with the sudden refraction of the QCM response during the cooling below the temperature of point 2.

As predicted, the sudden refraction of the resonant frequency shift (ΔF) at the temperature of point 2 was due to different working temperatures for the viscous and elastic friction in terms of vibrational loss. That is, although the viscous friction varied across the whole temperature range, the elastic friction only occurred below a certain temperature (point 2) with the formation of solid crystals. Thus, the temperature (point 2) at which elastic friction was initiated was in effect the induction point of primary nucleation in the SMZ solution (20 g/L). In reality, the clear SMZ solution suddenly changed to a milky white turbid suspension at the temperature of point 2. In addition, it should be noted that the predicted discontinuity in the resonant frequency shift (ΔF) at point 2 was due to a mismatch between the saturated temperature of the SMZ solution (20 g/L) and the temperature at which elastic friction was initiated, which resulted from the metastability of the supercooled solution.

After 30 min of stabilization at 25 °C, the crystal suspension was subjected to a reverse heating process (temperature of point 3), which meant that the crystals started to dissolve. As a result, the resonant frequency rapidly increased due to the decreased viscosity and dissolution of the solid mass on the sensor when increasing the temperature. This resonant frequency profile was then suddenly refracted at the temperature of point 4 due to the complete dissolution of the solid mass on the sensor. That is, below the temperature of point 4, the resonant frequency ($\Delta F = \Delta F_m + \Delta F_l$) was based on a combined contribution of the elastic (ΔF_m) and viscous frictions (ΔF_l), as predicted in Supporting Information (Figure S-2). However, above the temperature of point 4, the contribution of the elastic friction disappeared due to the complete dissolution of the crystals, leaving only the viscous friction (ΔF_l) contribution to the resonant frequency shift ($\Delta F = \Delta F_l$). Therefore, this refraction point was determined as the saturated point (saturated temperature). In reality, the turbid suspension became clear at this point. It should also be mentioned that no discontinuity in the resonant frequency shift was predicted due to the absence of metastability in the heating process.

During the cooling and heating cycle of the blank solution, no refraction of the frequency resonant shift occurred due to the absence of any solid crystal formation or dissolution. Thus, the resonant frequency shift (ΔF) uniquely depended on the viscous friction (ΔF_l) across the whole temperature range.

F−R Diagram Analysis. When the resonant frequency (F) and resonant resistance (R) on a time scale (F−t plot and R−t plot) were converted to a resonant frequency versus resonant resistance plot (F−R plot). F−R plot was first applied to interpret the phase transition phenomena of Langmuir−Blodgett films by Muramatsu et al. as shown in Figure 2a,[25] which is a quantitative pattern of viscosity change and elasticity change. The detail interpretation can be found in further applications of F−R plot.[37−39] Briefly, the shift of the QCM response from a → b → c → d in the F−R plot represents the increase of the viscous friction on the sensor. Thus, the F−R plot infers that the viscosity of the solution varied both the resonant frequency and the resonant resistance simultaneously. If the solution is viscoelastic, the shifting pathway of the F−R plot will deviate from a diagonal shift (a → b → c → d) due to the simultaneous contribution of viscous and elastic friction to the resonant frequency and resonant resistance. As a result, the slope will decrease when increasing the elasticity of the solution, resulting in a horizontal pathway of b → e → f if the film is purely elastic.

The resonant frequency and resonant resistance in Figure 1b were replotted on an F−R diagram, as shown in Figure 2b. When cooling the SMZ solution, the F−R plot initially showed a simple path of increasing viscosity (B → C in curve I). Suddenly at point C, the QCM response shifted almost horizontally, similar to the purely elastic response B → E → F in Figure 2a, due to spontaneous crystal nucleation. That is, the nucleation process generated an elastic solid mass of SMZ on the sensor, causing a significant increase of elastic friction without any change of the viscous friction. Thus, point C indicates the induction of primary nucleation, equivalent to point 2 in the F−t plot (Figure 1b). This result matched well with the analysis of the QCM responses for the cooling crystallization.[33]

During the heating of the SMZ suspension, the QCM response shifted from D′ → C′ → B′ on the F−R plot (curve III), where the slope of D′ → C′ deviated from the diagonal path (A → B or B′ → A′) due to the simultaneous contribution of the viscous and elastic frictions. That is, when increasing the temperature, the viscosity of the solution was reduced, while the solid crystals on the sensor were dissolved out. However, a further increase in the temperature shifted the QCM response to a pure viscosity change C′ → B′, indicating that the environment of the sensor was suddenly changed from a viscoelastic solution to a purely viscous solution at point C′, which corresponded to the saturated point (point 4 in Figure 1b). In the curve III, the QCM response shift from C″ → B″ having the same F−R slope with B″ → A″ represented the purely viscous environment of the sensor because of no solid formation in the blank solution.

DOI: 10.1021/ac504492g
Anal. Chem. 2015, 87, 3329−3335

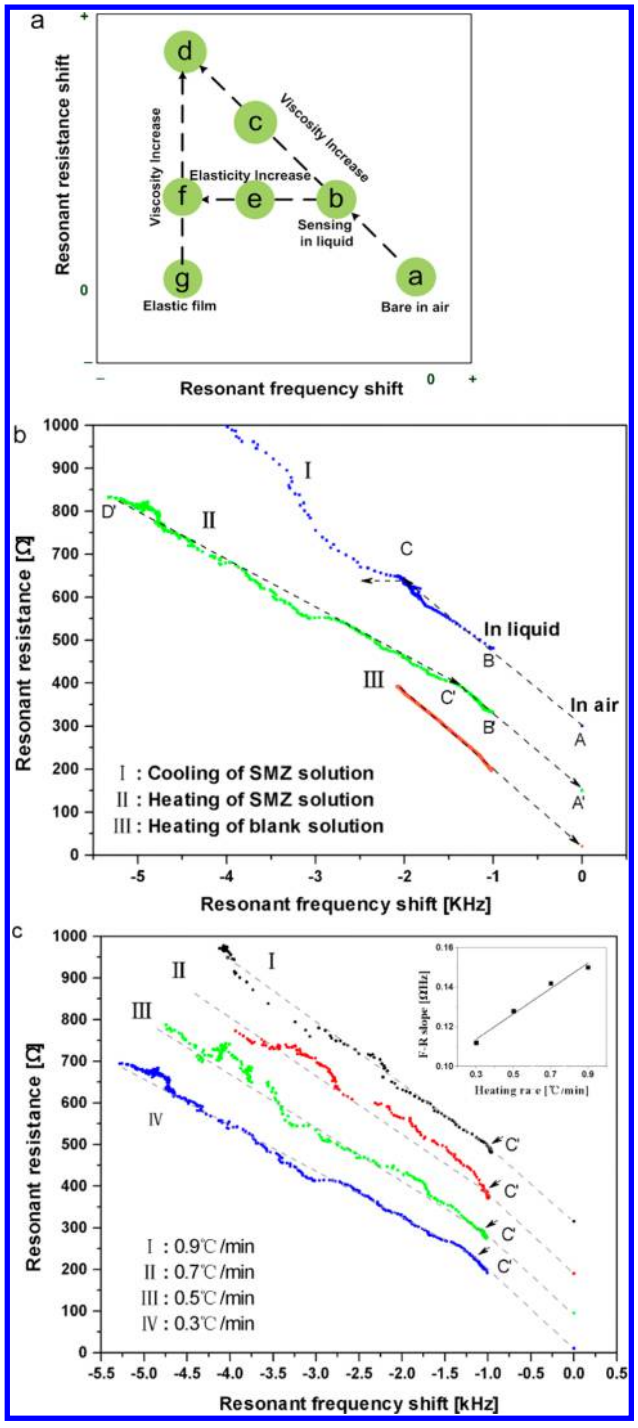

Figure 2. (a) *F*−*R* model of QCM: quantitative analysis of viscoelasticity of working film on sensor. (b) Analysis of *F*−*R* slope during cooling of 20g/l solution (I), heating of 20g/l solution (II), and heating of blank solution (III). (c) *F*−*R* plots of heating of 20g/l solution with heating rate of 0.9 °C/min (I), 0.7 °C/min (II), 0.5 °C/min (III), 0.3 °C/min (IV). Inset shows dependence of *F*−*R* plot slope on heating rate.

The effect of the heating rate on the dissolution of the crystals was also investigated, as shown in Figure 2c. Here, the SMZ concentration was fixed at 20g/l. When increasing the heating rate from 0.3 °C/min to 0.9 °C/min, the slope of the QCM response path D′ → C′ in the *F*−*R* plot was varied from −0.11 to −0.15. However, the turning point (point C′) from a viscoelastic medium to a viscous medium was almost invariant to the heating rate, suggesting that the QCM response to a heating dissolution process can provide a reliable and consistent value for the saturated concentration (solubility), regardless of the measuring conditions.

Accuracy and Reliability of QCM Responses. The accuracy and reproducibility of the QCM responses for determining the solubility were analyzed in comparison with the FBRM responses, which were based on scanning the solid particles in the solution. Thus, the crystal formation and dissolution during the cooling and heating processes are reflected in the FBRM particle counts shown in Figure 3. As

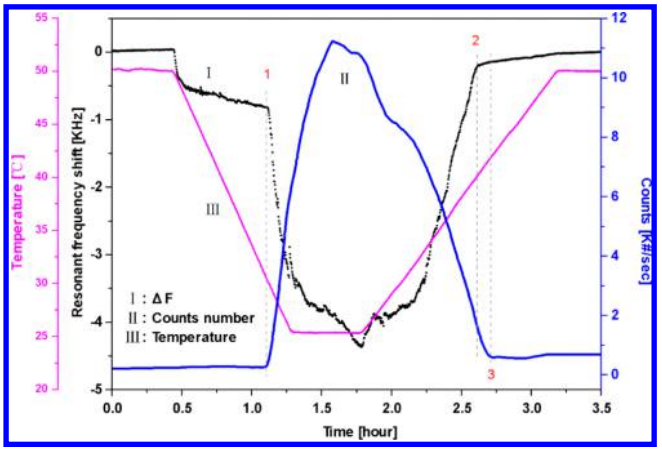

Figure 3. *In situ* analysis of cooling and heating of 20g/l solution: resonant frequency shift of QCM (I); particle number measured by FBRM (II); and temperature profile (III).

such, when cooling the solution, the flat profile of the particle counts was suddenly refracted at point 1 (in Figure 3.) due to the induction of crystal nucleation. With further cooling, the particle count sharply increased due to further high nucleation. This induction point measured by FBRM exactly matched the QCM response.

In the ensuing heating process, the particle count was reduced due to the dissolution of the crystals. Thus, another refraction of the particle count profile occurred at the saturated point (point 3 in Figure 3), at which point the crystals in the suspension were completely dissolved out. However, there was a small difference in the saturated points measured by FBRM (point 3 in Figure 3) and QCM (point 2 in Figure 3) due to the difference in their detection mechanisms.

To evaluate the reliability and consistency of the results, the QCM and FBRM responses were also examined when varying the heating rate at a fixed SMZ concentration (20 g/L), as shown in Figure 4. According to the QCM responses, when varying the heating rates, the saturated temperature was estimated at 40.7 ± 0.2 °C (Figure 4a). However, the FBRM responses estimated the saturated temperature at 43.3 ± 1.2 °C (Figure 4b). Here, it should be mentioned that the determination of the saturated temperature from the QCM responses slightly changed from 40.4 to 40.9 °C when varying the heating rate from 0.3 °C/min to 0.7 °C/min, whereas the determination from the FBRM responses showed a more significant change from 42.0 to 44.5 °C. Therefore, this result suggests that the QCM method for determining the saturated temperature is more reproducible and less sensitive to the measuring conditions than the FBRM method.

The saturated temperatures determined by the QCM and FBRM responses at various SMZ concentrations were

DOI: 10.1021/ac504492g
Anal. Chem. 2015, 87, 3329−3335

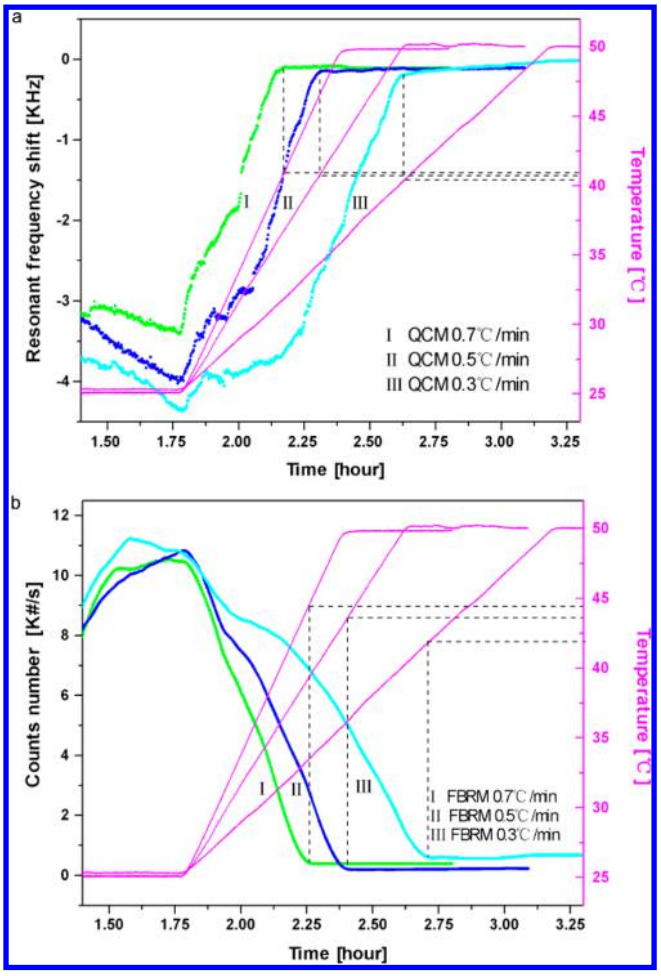

Figure 4. Heating of 20g/l solution at various heating rate of 0.7 °C/min (I), 0.5 °C/min (II), and 0.3 °C/min (III) monitored by QCM (a) and FBRM (b).

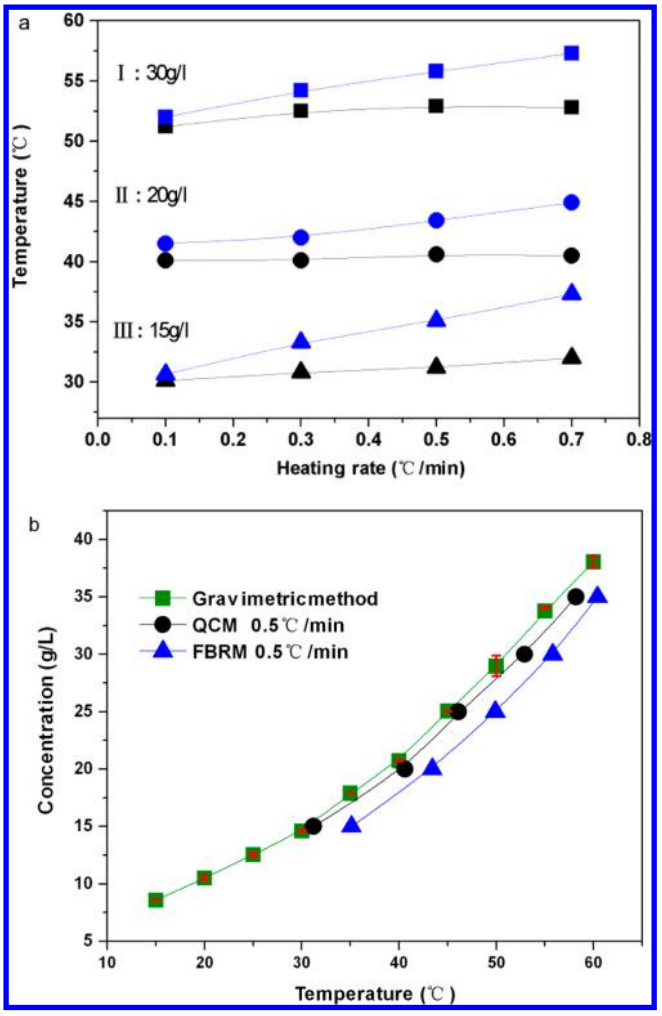

Figure 5. (a) Effect of heating rate on saturated temperature determined by FBRM (blue) and QCM (black). (b) Comparison of solubility determined by gravimetric method (green), QCM (black), and FBRM (blue).

compared, as shown in Figure 5a. Although the QCM saturated temperature was almost independent of the heating rate at all solution concentrations, the FBRM saturated temperature increased significantly when increasing the heating rate. Thus, at a low heating rate of 0.1 °C/min, the saturated temperatures determined by QCM and FBRM were close within 1.0 °C; however, this gap increased to over 5 °C when increasing the heating rate to 0.7 °C/min. This difference between the saturated temperatures may have originated from the different working principle of the instruments detecting the property change of the medium, where an overshoot of FBRM is probable based on the consistently higher saturated temperature.

The accuracy of the QCM and FBRM methods was evaluated in comparison with the solubility measured using a thermogravimetric method (Figure 5b and Table 1). Here, the gravimetric method was repeated at least three times to create a reference solubility. As shown in Figure 5b, the solubility determined by the QCM responses at 0.5 °C/min was quite close to the reference, within 1 °C for the whole temperature range, whereas the solubility determined by the FBRM responses deviated significantly from the reference, over 4 °C. The accuracy of the QCM solubility is summarized in Table 1. Here, the error was defined as the relative difference between the determined values (QCM and FBRM methods) and the reference values (gravimetric method). The QCM method only showed random errors within 4% for all the heating rates. However, the FBRM method showed much higher errors of over 16% according to the heating rate. Therefore, the QCM method was highly accurate and reliable with simplicity in determining the solubility.

CONCLUSION

The QCM method was shown to be effective for determining the solubility. The QCM sensor was highly sensitive to environmental changes, such as the viscosity of the solution and solid mass (1.0 ng/Hz). Subtle changes in the solution viscosity (viscous friction) and solid mass (elastic friction) on the sensor during the cooling and heating of the SMZ solution were sensitively reflected in the QCM responses of the resonant frequency and resonant resistance. During the cooling of the SMZ solution, the viscous friction continuously increased for the whole temperature range, resulting in the decrease of the resonant frequency and increase of the resonant resistance. However, the elastic friction to the QCM responses was only added when the solution was cooled below the induction temperature, at which point the resonant frequency was suddenly refracted.

DOI: 10.1021/ac504492g
Anal. Chem. 2015, 87, 3329−3335

Table 1. Accuracy Evaluation of Solubility Determination

		QCM						FBRM					
	gravimetric method	0.1 °C/min		0.3 °C/min		0.5 °C/min		0.1 °C/min		0.3 °C/min		0.5 °C/min	
C (g/l)	T_S (°C)	T_S(°C)	error (%)	T_S(°C)	error (%)	T_S(°C)	error (%)	T_S(°C)	error (%)	T_S(°C)	error (%)	T_S(°C)	error (%)
15	30.2	30.1	−0.331	30.8	1.986	31.2	3.311	30.65	1.490	33.3	10.26	35.1	16.225
20	38.8	40.1	3.35	40.1	3.350	40.6	4.639	41.5	6.958	42	8.247	43.4	11.855
25	45.1	46.5	3.104	46.8	3.769	46.1	2.217	47.1	4.434	49.1	8.869	49.9	10.643
30	51.1	51.2	0.195	52.5	2.739	52.9	3.522	52.0	1.761	54.2	6.066	55.8	9.197
35	56.3	56.8	0.888	57.25	1.687	58.2	3.374	57.6	2.309	59.4	5.506	60.4	7.282

The values from the gravimetric method were counted as reference. Error = (measured value − reference value)/reference × 100%.

During the reverse heating process, the QCM responses were inversed. When heating the suspension, the viscosity of the solution decreased, and the solid crystals loaded on the sensor were dissolved, resulting in a rapid increase of the resonance frequency and corresponding decrease of the resonant resistance. After the complete dissolution of the solid crystals loaded on the sensor above the saturated temperature, the resonant frequency became solely dependent on the viscous friction.

Because the QCM method is simultaneously based on the property changes in the solution and solid phases, the determination of the induction and saturated temperatures were almost invariant and highly consistent when varying the cooling and heating rates. A comparison with the results from FBRM and gravimetric methods also confirmed that the QCM method was accurate and reliable in determining the induction and saturated temperatures. Therefore, it was concluded that the QCM method is a highly promising technique for detecting the equilibrium (solubility) and dynamic (crystal nucleation) states with minimal effort based on simple temperature cycling, thereby avoiding calibration and sampling.

■ ASSOCIATED CONTENT

Supporting Information

Solubility determination using thermogravimetric method, response of resonant frequency shift to working material, and prediction of resonant frequency shift. This material is available free of charge via the Internet at http://pubs.acs.org.

■ AUTHOR INFORMATION

Corresponding Author

*E-mail: wskim@khu.ac.kr. Tel.: +82 31 201 2970. Fax: +82 31 273 2971.

Notes

The authors declare no competing financial interest.

■ ACKNOWLEDGMENTS

This work was supported by NRF grant funded by MSIP, Korea, (2010-0017993) and (Grant NRF-2014-009799).

■ REFERENCES

(1) Saal, C.; Petereit, A. C. *Eur. J. Pharm. Sci.* **2012**, *47*, 589−595.
(2) Bhattachar, S. N.; Deschenes, L. A.; Wesley, J. A. *Drug Discovery Today* **2006**, *11*, 1012−1018.
(3) Borissova, A.; Khan, S.; Mahmud, T.; Roberts, K. J.; Andrews, J.; Dallin, P.; Chen, Z. P.; Morris, J. *Cryst. Growth Des.* **2009**, *9*, 692−706.
(4) Groen, H.; Roberts, K. J. *Cryst. Growth Des.* **2004**, *4*, 929−936.
(5) Hu, Y. R.; Liang, J. K.; Myerson, A. S.; Taylor, L. S. *Ind. Eng. Chem. Res.* **2005**, *44*, 1233−1240.
(6) Hoelke, B.; Gieringer, S.; Arlt, M.; Saal, C. *Anal. Chem.* **2009**, *81*, 3165−3172.
(7) Fujiwara, M.; Chow, P. S.; Ma, D. L.; Braatz, R. D. *Cryst. Growth Des.* **2002**, *2*, 363−370.
(8) Zhang, X. Y.; Wang, X. F.; Hao, L.; Yang, X. W.; Dang, L. P.; Wei, H. Y. *Cryst. Res. Technol.* **2012**, *47*, 1153−1163.
(9) Sapoundjiev, D.; Lorenz, H.; Seidel-Morgenstern, A. *Thermochim. Acta* **2005**, *436*, 1−9.
(10) Carless, J. E.; Swarbrick, J. *J. Pharm. Pharmacol.* **1964**, *16*, 633−634.
(11) Reviakine, I.; Johannsmann, D.; Richter, R. P. *Anal. Chem.* **2011**, *83*, 8838−8848.
(12) Mecea, V. M. *Sens. Actuators, A* **2006**, *128*, 270−277.
(13) Lu, J. L.; Liu, B.; Greeley, J. P.; Feng, Z. X.; Libera, J. A.; Lei, Y.; Bedzyk, M. J.; Stair, P. C.; Elam, J. W. *Chem. Mater.* **2012**, *24*, 2047−2055.
(14) Kang, H. W.; Lee, D. Y.; Muramatsu, H.; Lee, B. J.; Kwon, Y. S. *J. Nanosci. Nanotechnol.* **2011**, *11*, 4236−4239.
(15) Turon, X.; Rojas, O. J.; Deinhammer, R. S. *Langmuir* **2008**, *24*, 3880−3887.
(16) Guo, H. S.; Kim, J. M.; Chang, S. M.; Kim, W. S. *J. Nanosci. Nanotechnol.* **2009**, *9*, 2937−2943.
(17) Guo, H. S.; Kim, J. M.; Chang, S. M.; Kim, W. S. *Biosens. Bioelectron.* **2009**, *24*, 2931−2934.
(18) Guo, H. S.; Kim, J. M.; Kim, S. J.; Chang, S. M.; Kim, W. S. *Langmuir* **2009**, *25*, 648−652.
(19) Kim, J. M.; Chang, S. M.; Li, F.; Guo, H. S.; Kim, W. S. *J. Nanosci. Nanotechnol.* **2011**, *11*, 7676−7681.
(20) Hao, R. Z.; Song, H. B.; Zuo, G. M.; Yang, R. F.; Wei, H. P.; Wang, D. B.; Cui, Z. Q.; Zhang, Z. P.; Cheng, Z. X.; Zhang, X. E. *Biosens. Bioelectron.* **2011**, *26*, 3398−3404.
(21) Uludag, Y.; Tothill, I. E. *Anal. Chem.* **2012**, *84*, 5898−5904.
(22) Lee, H. S.; Contarino, M.; Umashankara, M.; Schon, A.; Freire, E.; Smith, A. B.; Chaiken, I. M.; Penn, L. S. *Anal Bioanal. Chem.* **2010**, *396*, 1143−1152.
(23) Zhang, S.; Bai, H.; Luo, J.; Yang, P.; Cai, J. *Analyst* **2014**, *139*, 6259−6265.
(24) Arenas, K. J. L.; Schill, S. R.; Malla, A.; Hudson, P. K. *J. Phys. Chem. A* **2012**, *116*, 7658−7667.
(25) Muramatsu, H.; Kimura, K. *Anal. Chem.* **1992**, *64*, 2502−2507.
(26) Zhu, X. L.; Yang, J. H.; Liu, M.; Wu, Y.; Shen, Z. M.; Li, G. X. *Anal. Chim. Acta* **2013**, *764*, 59−63.
(27) Wang, W.; Deng, Y.; Li, S.; Liu, H. N.; Lu, Z. X.; Zhang, L. M.; Lin, L.; Xu, L. J. *J. Biomed. Nanotechnol.* **2013**, *9*, 736−740.
(28) Deng, Y.; Wang, W.; Ma, C.; Li, Z. Y. *J. Biomed. Nanotechnol.* **2013**, *9*, 1378−1382.
(29) Deng, Y.; Wang, W.; Zhang, L. M.; Lu, Z. X.; Li, S.; Xu, L. J. *J. Biomed. Nanotechnol.* **2013**, *9*, 318−321.
(30) Kashefi-Kheyrabadi, L.; Mehrgardi, M. A.; Wiechec, E.; Turner, A. P. F.; Tiwari, A. *Anal. Chem.* **2014**, *86*, 4956−4960.
(31) Pan, Y. L.; Guo, M. L.; Nie, Z.; Huang, Y.; Pan, C. F.; Zeng, K.; Zhang, Y.; Yao, S. Z. *Biosens. Bioelectron.* **2010**, *25*, 1609−1614.
(32) Zhang, S.; Bai, H.; Luo, J.; Yang, P.; Cai, J. *Analyst* **2014**, *139*, 6529−6265.
(33) Yao, C. Y.; Qi, Y. Z.; Zhao, Y. H.; Xiang, Y.; Chen, Q. H.; Fu, W. L. *Biosens. Bioelectron.* **2009**, *24*, 2499−2503.

DOI: 10.1021/ac504492g
Anal. Chem. 2015, 87, 3329−3335

(34) Liu, L.-S.; Kim, J.; Chang, S.-M.; Choi, G. J.; Kim, W.-S. *Anal. Chem.* **2013**, *85*, 4790−4796.
(35) Sauerbrey, G. *J. Z. Phys.* **1959**, *155*, 206−222.
(36) Kanazawa, K. K.; G, J. G. *J. Anal. Chim. Acta.* **1985**, *175*, 99−105.
(37) Kim, J. M.; Chang, S. M.; Muramatsu, H.; Isao, K. *Korean J. Chem. Eng.* **2011**, *28*, 987−1008.
(38) Muramatsu, H.; Kim, J. M.; Chang, S. M. *Anal. Bioanal. Chem.* **2002**, *372*, 314−321.
(39) Muramatsu, H.; Tamiya, E.; Karube, I. *Anal. Chem.* **1988**, *60*, 2142−2146.

DOI: 10.1021/ac504492g
Anal. Chem. 2015, 87, 3329−3335